Geologie en Mijnbouw 65: 119–132 (1986)

Dynamical aspects of active continental margins

M.J.R. Wortel
Department of Theoretical Geophysics, Institute of Earth Sciences, University of Utrecht, P.O. Box 80.021, 3508 TA Utrecht, The Netherlands

Received 16 April 1986; accepted in revised form 30 May 1986

Abstract

Many tectonic processes along active continental margins (and convergent plate boundaries, in general) are closely related to the dynamics of the subduction process. A major force associated with the subduction of oceanic lithosphere is the slab pull, the result of the density contrast between the cold and dense descending slab and the surrounding warmer mantle. This force is generally assumed to be compensated by resistive forces acting on the slab. In this paper I emphasize that such a compensation may be valid for a plate's convergent boundary as a whole but certainly not always for each segment of the trench system. Stress may be transmitted from the subducted slab to the attached lithospheric plate at the surface, and taking this into account provides insight into the relationship between upper mantle processes and tectonic processes near the surface (e.g. fragmentation of plates, accretion of sediments at trenches, and vertical tectonics of active continental margins).

Introduction

Early studies of the dynamics of plate motion (Elsasser 1967, McKenzie 1969) already recognized the slab pull to be a major force responsible for and maintaining the motion of lithospheric plates. This force arises from the temperature contrast – and, hence, via thermal contraction the density contrast – between the cold descending slab in a subduction zone and the warmer upper mantle surrounding the slab. Thus, the dense subducted slab may be considered to sink under its own weight, pulling the attached plate towards the trench. Subsequent quantitative investigations by Forsyth & Uyeda (1975), Chapple & Tullis (1977) and Backus et al. (1981) have confirmed this early assessment.

Another conclusion of these three studies was that the slab pull is balanced – or very nearly so – by the resistive shearing forces acting on the downgoing slab. If such a balance would apply locally, it would mean that, albeit the high magnitude of the slab pull, very little of this force is transmitted to the attached horizontal part of the plate. Consequently, the slab pull would have little or no effect on geodynamic processes near the surface. Several authors, including Forsyth & Uyeda (1975) and (especially) Chapple & Tullis (1977), have pointed out, however, that the compensation of the slab pull by the resistive forces should not be taken to apply for each segment of a convergent plate boundary (subduction zone), but rather for a subducting plate boundary as a whole.

Insight gained by studying the role of lithospheric age in the subduction process (Vlaar 1975, Vlaar & Wortel 1976, Wortel & Vlaar 1978, Wortel 1980, 1982, 1984, England & Wortel 1980)

has brought out the significance of a (partially) uncompensated or over-compensated slab pull force. The extent to which the slab pull force is compensated may vary considerably along a convergent plate boundary, thus giving rise to laterally varying boundary forces acting on the (non-subducted) lithosphere. This, in turn, strongly affects the stress field in the lithosphere.

In this paper I will show that taking into account an unbalanced slab pull contributes to a better understanding of several tectonic processes at or near the surface, in particular in the vicinity of the trenches along convergent plate boundaries.

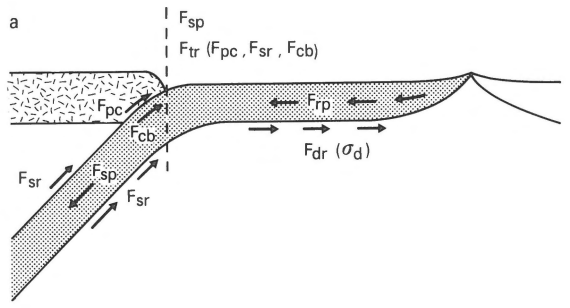

Fig. 1. Schematic representation of the main forces acting on a subducting oceanic plate. Driving forces: F_{rp} (ridge push) and F_{sp} (slab pull). Resistive forces: F_{dr} (drag force at the base of the plate; σ_d is shear stress), F_{tr} (resistance at the trench and in the subduction zone). F_{tr} is composed of three parts: F_{cb} (compositional buoyancy), F_{pc} (resistance at the plate contact) and F_{sr} (slab resistance by viscous shearing forces along the slab/upper-mantle interfaces).

Dynamics of subduction

To place the problem of compensation of the slab pull force into the more general perspective of the dynamics of the lithosphere this section starts with a short sub-section on plate tectonic forces. The importance of the age of the descending lithosphere for the dynamics of the subduction process is stressed in a second sub-section on age-dependent subduction.

Plate tectonic forces

In this sub-section I focus on the instructive case of a spreading and subducting oceanic plate. With some rather straightforward modifications the analysis can be generalized to include continental lithosphere. The main forces acting on a spreading and subducting oceanic plate are indicated in Fig. 1.

The forces which drive the plates are the ridge push F_{rp} and the slab pull F_{sp}. The ridge push force is not a boundary force acting at the ridge axis but a pressure gradient intergrated over the area of the plate (Lister 1975). This pressure gradient results from the cooling and densification of the lithosphere. Therefore, contributions to the ridge push come from all parts of the oceanic lithosphere which are subject to continued cooling, that is all oceanic lithosphere younger than approximately 100 Ma. The other driving force, the slab pull F_{sp}, results from the density contrast between the cold descending slab and the surrounding warmer upper mantle (e.g. Elsasser 1967, McKenzie 1969).

The resistive forces shown in Fig. 1 are the drag force acting at the base of the lithosphere (that is the shear stress σ_d integrated over the area of the base of the plate) and the resistive forces F_{tr} acting on the downgoing slab in the trench region and in the upper mantle part of the subduction zone. The latter forces consist of the compositional buoyancy force F_{cb} and resistive shearing forces F_{pc} (the integrated value of the shear stress σ_{pc} along the plate contact with the overriding plate) and F_{sr} (the integrated value of σ_{sr}, the resistance to slab penetration in the upper mantle by viscous shearing forces). F_{cb} is associated with the petrological stratification of the oceanic crust and upper mantle created during the spreading process (Vlaar & Wortel 1976, Oxburgh & Parmentier 1977). The density structure of the layering contributes a gravitationally stable component to the lithosphere/asthenosphere system. Upon subduction this is felt as a force (F_{cb}) which counteracts the gravitationally unstable component resulting from the cooling and densification of the lithosphere which is represented by F_{sp}.

In specific cases, different from the entirely oceanic plate considered here and therefore not indicated in Fig. 1, some other forces may be rele-

vant, like drag beneath the continents and the forces associated with continental collision (see Cloetingh & Wortel 1985, 1986).

Age-dependent subduction

Information for this section is drawn from a global study of the subduction process (see Wortel 1980, 1982) which included all subduction zones for which adequate data on slab geometry (length, dip and maximum depth of the seismic zone), relevant plate kinematics and age of the downgoing slab were available.

For the subduction process the significant age of downgoing lithosphere is the age at the time it arrived at the trench and started to descend, since this equals the length of the period during which it has been cooling after formation at a spreading centre.

Fig. 2 shows the resorption times of the lithospheric slabs in the various subduction zones as a function of age. The resorption time t_{res} is defined as the downdip length of the seismic zone (S_{sz}, measured from the surface to the depth of the deepest earthquake foci) divided by the convergence rate normal to the plate contact (v_c). The graph shows a strong increase in resorption time with the age of the downgoing lithosphere. This can be approximated by a linear relationship for the resorption time:

$$t_{res} = (0.12 \pm 0.03) \cdot \text{age} \qquad (1)$$

Thus, the downdip length of the seismic zone is given by

$$S_{sz} = (0.12 \pm 0.03) \cdot v_c \cdot \text{age} \qquad (2)$$

Note that the maximum observed resorption time is 15 Ma.

Thermal model calculations have been carried out (Wortel 1980, 1982) on the basis of McKenzie's (1969) model in which a slab is assumed to sink through a mantle with an adiabatic temperature gradient. The adiabatic temperature distribution in the upper mantle below the lithosphere corresponds to a constant potential temperature T_m^p here taken as 1200° C. Potential temperature may be

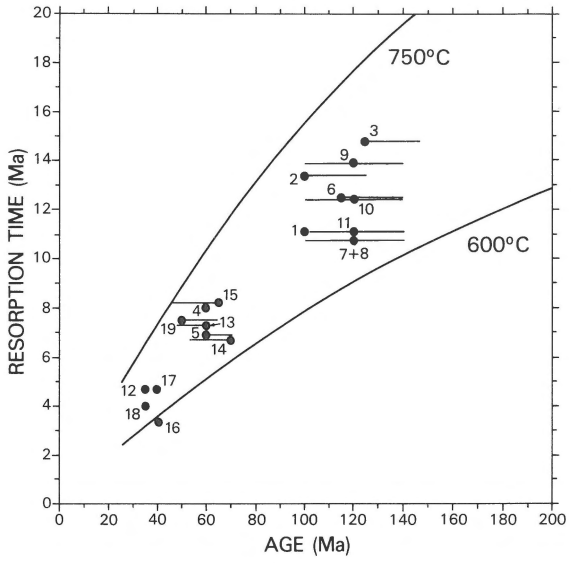

Fig. 2. Resorption times of subducted oceanic lithosphere as a function of lithospheric age. The symbols indicate the resorption times for the following zones: 1, Kuriles; 2, N. Honshu; 3, Izu-Bonin; 4, Ryukyus; 5, Sumatra; 6, Java; 7, Tonga (20° S); 8, Tonga (24° S); 9, Kermadec (28° S); 10 and 11, New Zealand; 12, Chile (36–42° S); 13, Chile (27–33° S); 14, Chile (18–26° S); 15, North-central Peru; 16, Central America 87° W); 17, Central America (90° W); 18, Alaska (150° W); 19, Aleutians (180° W). Bars on only one side of the symbols indicate temporal variations in age: the symbols are plotted at the estimated age at which the deepest part of the seismic zone (of the subducted slab) started to descend. The other end of the bar indicates the present age of the lithosphere at the trench. Two-sided bars are used for some zones in which the age of the descending lithosphere may vary between 100 and 140 Ma. The two curves indicate the resorption time (that is, the maximum downdip penetration divided by the convergence rate) of two isotherms of potential temperature.

regarded as the real temperature minus the effect of adiabatic compression and the contribution of latent heat from phase changes (McKenzie 1970). In Fig. 2 the values of $x_{max}^{(i)}/v_c$, where $x_{max}^{(i)}$ is the maximum downdip penetration of an isotherm of potential temperature, are plotted for the 600° C and 750° C isotherms. It follows that the downdip ends of seismic zones in subducted slabs are characterized by minimum potential temperatures between 600° C and 750° C.

Fig. 3 displays the maximum focal depths of earthquakes in subducted slabs as a function of lithospheric age. This relation has been established

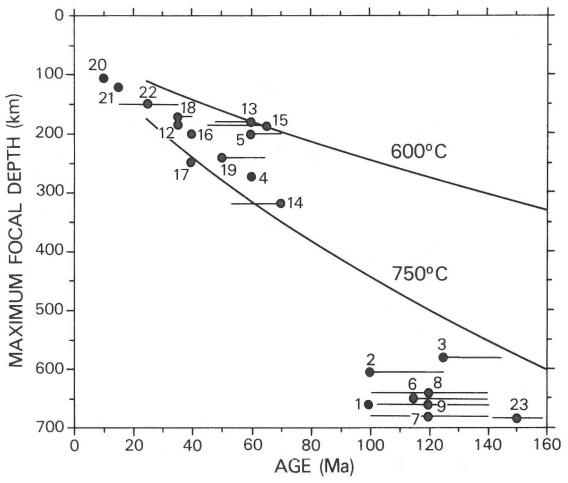

Fig. 3. Maximum focal depth of earthquakes in subduction zones as a function of the age of the subducted lithosphere. Symbols and numbers are the same as in Fig. 2, with the addition of 20, Cascades; 21, Chile (42–46° S); 22, Mexico (102° W); 23, Marianas (these zones could not be included in Fig. 2 owing to great uncertainties in v_c and in down-dip length of the seismic zone). The penetration depths of the 600° C and the 750° C isotherms of potential temperature are plotted for a vertical velocity v_z = 2.5 cm/yr.

by Vlaar & Wortel (1976). Only subduction zones in which lithosphere older than 70–100 Ma is consumed exhibit deep focus earthquakes. The depth-age relations for the 600° C and the 700° C isotherms were calculated for an average sinking rate v_z of 2.5 cm/yr. All data points in Fig. 2, with the exception of point 16, are bounded by the two isotherms. In Fig. 3 this is only the case for ages below 70 Ma. This means that the sinking rate v_z = 2.5 cm/yr is appropriate for these ages but clearly too low for ages above 70–100 Ma. For lithosphere of these ages the sinking rate appears to be between 4 and 6 cm/yr.

Compensation of the slab pull: partial or complete?

To answer the above question we consider the dependence of the slab pull on the various pertinent parameters.

The slab pull F_{sp} is the downdip component of the gravitational body force acting on the dense subducted slab. Per unit of length in the direction of the trench this can be expressed as:

$$F_{sp} = g \sin\varphi \int_0^L \int_o^{S_{sz}} \Delta\varrho \, dxdz \qquad (3)$$

Here, g is the gravitational acceleration, φ the dip and L the thickness of the downgoing slab, and $\Delta\varrho$ the density contrast between slab and surrounding mantle. The x- and z- directions are downdip and vertical to the upper (dipping) interface between the slab and the upper mantle, respectively. The downdip integration is limited to the end of the seismic zone (S_{sz}), which is reasonable in view of the drastic change in constitution (rheology) and subsequent deformation beyond this point (see Wortel 1986). Using McKenzie's (1969) thermal model we find

$$F_{sp} = \frac{4g\alpha\varrho_m T_m L^3}{\varkappa\pi^4} v_c \sin\varphi \, [1\text{-}\exp(-\frac{\pi^2\varkappa S_{sz}}{v_c L^2})] \qquad (4)$$

The parameters α, ϱ_m, T_m and $\varkappa$ are the coefficient of thermal expansion, the density and the temperature of the asthenosphere, and the thermal diffusivity of the asthenosphere/lithosphere. For the present purpose, all these parameters may be taken to be constant. The thickness L of the lithosphere increases with age t according to a square-root-of-age relation, at least for t<70 Ma (see Wortel 1980 for a review). Using this age-dependence of L, the relation (2) and $\varkappa = 0.9 \times 10^{-6}$ m^{2}s^{-1} we obtain

$$[1\text{-}\exp(-\frac{\pi^2\varkappa S_{sz}}{v_c L^2})] = 0.29$$

Thus, the factor between brackets in (4) does depend neither on v_c nor on the age of the lithosphere. Putting $v_c \sin\varphi = v_z$, it is found that

$$F_{sp} \propto v_z L^3 \qquad (5a)$$

Taking into account the above-mentioned age-dependence of L gives

$$F_{sp} = c_{sp} \, v_z \, t^{3/2} \qquad (5b)$$

where c_{sp} is a constant.

The resistive (viscous shearing) stress σ_{sr} along the slab/upper-mantle interface is taken to be proportional to the relative velocity of the slab and the upper mantle. Integrated along the downdip extent (S_{sz}) of the slab, this yields (again per unit width):

$$F_{sr} \propto v_c S_{sz} \quad (6a)$$

and, with (2):

$$F_{sr} = c_{sr} v_c^2 t \quad (6b)$$

where c_{sr} is a constant of proportionality

Combining the forces on the slab, all per unit width in the direction of the strike of the trench, we obtain the net force in the trench region exerted by the slab on the horizontal part of the plate. This net force, designated by F_{nt}, acts on the cross section of the plate indicated by the dashed line in Fig. 1. Positive values of F_{nt} – and of the other forces – correspond with forces directed from the ocean towards the trench. Hence, negative values correspond with resistance to continuing subduction. Thus, the net force is

$$F_{nt} = F_{sp} - (F_{cb} + F_{pc} + F_{sr}) \quad (7a)$$

or

$$F_{nt} = c_{sp} v_z t^{3/2} - (F_{cb} + F_{pc} + c_{sr} v_c^2 t) \quad (7b)$$

It should be noted that v_z can vary with the age of the lithosphere (according to the relation discussed for Fig. 3), whereas v_c can not. v_c depends on the dynamics of the two converging plates: it cannot simply adjust to the age of the downgoing slab at a certain segment of the trench.

So far, I have taken the compositional buoyancy force F_{cb} and the shear resistance at the plate contact F_{pc} to be independent of age. For the former force this is a sound assumption because the density variations due to composition are not likely to vary significantly with time and age (see Oxburgh & Parmentier 1977 and England & Wortel 1980). As to the latter force, there is strong evidence from seismological studies that the coupling between the downgoing plate and the overriding plate decreases with the age of the slab (Ruff & Kanamori 1980). This would imply a decrease in F_{pc} with age. From (7b), and in particular from the difference in the age-dependences of the driving and the resistive forces, it follows that the net force is clearly a function of the age of the downgoing lithosphere. Starting from a value smaller (in magnitude) than the resistive forces, the driving force grows faster with age than the resistive forces do. The probable decrease of F_{pc} with age even strengthens this trend. Thus, qualitatively, F_{nt} is negative for young lithosphere (over-compensation, implying resistance to continuing subduction) and positive for old lithosphere (partial compensation). The transition between negative and positive F_{nt} takes place at an age of about 40 Ma. This relationship can be quantified further by using the results of England & Wortel (1980).

The relation between F_{nt} and lithospheric age should not be interpreted as being contradictory to the result obtained by Cloetingh (1982). His result, implying that initiation of subduction is to be expected in young lithosphere rather than in old lithosphere, refers to the state of stress required to cause failure along a passive continental margin. It does not imply that young lithosphere is subducted more easily than old lithosphere.

The account given above serves to bring out some basic acpects of the dynamics of subduction. A more detailed discussion, however, is beyond the scope of the present paper. Instead I will now present the results of some investigations which clearly and quantitatively demonstrate the significance of age-dependent forces. In conclusion, on the basis of the analysis of the slab pull force and the forces counteracting the slab pull it appears that complete compensation should be considered as an exceptional situation rather than a common one.

Implications of the slab pull being uncompensated

Stress field in the lithosphere: general aspects

The plate tectonic forces considered above contribute to the state of stress in the lithosphere. In fact, their contribution generally outweighs those of other origins, such as thermal stresses and membrane stresses (see Cloetingh 1982 for a review). An exception to this are bending stresses in the lithosphere, for example near trenches along convergent plate boundaries (see below).

If F_{sp} were exactly balanced by resistive forces one could infer the stress in the oceanic lithosphere from a cross section such as shown in Fig. 1. Along these lines, and using their main conclusion – an

almost complete compensation of the slab pull F_{sp} by the viscous shearing force F_{sr} (see Fig. 1) – Forsyth & Uyeda (1975) predicted that the horizontal part of oceanic plates would be in a state of weak compressive stress because the ridge push F_{rp} is counteracted by the sum of the drag force F_{dr} and the resistance at the plate contact F_{pc}.

As Chapple & Tullis (1977) realized, the net subduction force (here denoted by F_{nt}) exerted on a plate from a long convergent plate boundary may give rise to intraplate stresses of considerable magnitude. On the basis of the force modelling discussed in the previous chapter I will now illustrate the importance of the slab pull for the intraplate stress field by discussing results of numerical models for the Nazca (and the Farallon) plate and the Indo-Australian plate, obtained by Wortel & Cloetingh (1981, 1983, 1985) and Cloetingh & Wortel (1985, in press).

With a rheological model for the lithosphere the stress field in the lithosphere associated with the plate tectonic forces can be calculated numerically. This field, which is called regional stress field, represents the non-lithostatic state of stress in the lithosphere. Because the stress values are to be compared with the strength distribution in the lithosphere – which is expressed in terms of differential stress – the lithostatic part of the stress field (depth-dependent pressure) can be omitted.

To ensure mechanical equilibrium, the net torque exerted by the forces on a plate is required to vanish:

$$\sum_{N} \int_{P} \bar{r} \times \bar{F} \, dp = 0 \qquad (8)$$

where the sum is over the total set of N forces and the integration over the boundaries or the area of the plate P, depending on the nature of the force involved (boundary force or surface force).

On the basis of their established age-dependence the driving forces F_{rp} and F_{sp} can be calculated. Several unknown parameters associated with the resistive forces can be determined from eq. (8) (see Wortel & Cloetingh 1981, 1983 and Cloetingh & Wortel 1985, in press).

The plates are modelled as being elastic, with a reference thickness of 100 km, Young's modulus $E = 7 \times 10^{10}$ Nm^{-2} and Poisson's ratio $\nu = 0.25$. From model results for this rheology the stresses in a plate with a more complex rheology (see Goetze & Evans 1979) can simply be derived.

Fragmentation of plates

Studies of marine magnetic anomalies have clearly shown that lithospheric plates can break up into two or more plates that move in divergent directions, thus giving rise to the formation of new spreading centres. A well-documented example of such a process is the fragmentation of the Farallon plate (the ancestor of the present-day Cocos plate and Nazca plate, see Fig. 5) which took place approximately 25–30 Ma ago (Hey 1977).

Using finite element methods and a reconstruction of regional plate boundaries Wortel & Cloetingh (1981, 1983) investigated the state of stress in the Farallon plate as it was approximately 25–30 Ma ago, to see whether the stress field provided a clue towards understanding the fragmentation. On the basis of a reconstructed age pattern in the Farallon plate, the established age-dependence of the driving forces F_{rp} and F_{sp}, and with the use of Eq. (8), the forces acting on the plate could be modelled. The intersections of the Pacific-Farallon spreading centre – the ancestor of the present East Pacific Rise – with the trench system (along the coast of present-day Mexico, Central and South America, see Fig. 5) imply variations in the age of the lithosphere at the trench. These variations lead to lateral variations along the trench in the net force F_{nt} associated with the subducting slab: negative values for F_{nt} (resistance) near the trench-ridge intersections (Baja California, Mexico and Southern Chile), and positive values for F_{nt} (driving force) in the central parts of the trench system. The basic features of this situation are represented in Fig. 4. Such lateral variations cause a sort of in-plane (horizontal) bending process in the plate.

The resulting stress field in the Farallon plate is shown in Fig. 5. It appears to be dominated by high tensional stresses, roughly parallel to the trench axis. Wortel & Cloetingh (1981, 1983) proposed

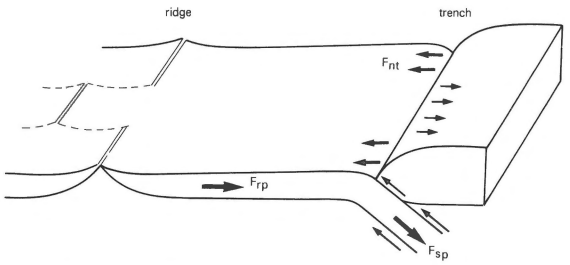

Fig. 4. Schematic diagram of a convergent plate boundary. F_{nt} represents the net force exerted by the downgoing slab on the attached oceanic plate. The direction of the force F_{nt} in the central part of the trench corresponds with a net force pulling the plate towards the trench. Differences in age of the subducted lithosphere, caused for example by a ridge configuration as shown, result in lateral variations in F_{nt} along the trench. The force distribution along the trench systems of the Farallon plate and the present-day Nazca plate ressembles the situation shown in this figure.

that the approximately North-South directed tensional stresses near present-day Panama and Colombia, resulting from lateral variations in F_{nt}Åt, have caused the fragmentation of the Farallon plate.

From the stress field in Fig. 5 no particular preference can be inferred for failure in the northernmost stippled region. Everywhere along the central part of the trench system high stresses prevail. If failure occurs in one part of the plate, however, the state of stress in the plate is relaxed, and the two new parts may change their rate and direction of motion. Their motion is no longer determined by the forces acting on all of the original plate but only by those acting on each of the smaller plates separately. The young lithosphere near the trench off northwest Mexico and southern Chile will cause the Cocos and Nazca plates to pivot around the intersections of the ridge and the trench. In this respect the postulated break-up region near present-day Panama and Colombia may have had some preference over other regions, because the new direction of the Cocos plate could easily be accommodated in the Central American trench system.

Wortel & Cloetingh (1983, 1985) also applied their modelling procedure to the present Nazca plate. In this case, again, the distribution of F_{nt} along the trench ressembles the schematic configuration of Fig. 4: positive values of F_{nt} in the central part of the trench system (between latitudes of about 17° S and 27° S) and negative values in the southern and northern parts of the trench system. The corresponding stress field in the Nazca plate is presented in Fig. 6: tensional stresses parallel to the trench can again be recognized, although the magnitudes are smaller than those of the Farallon plate.

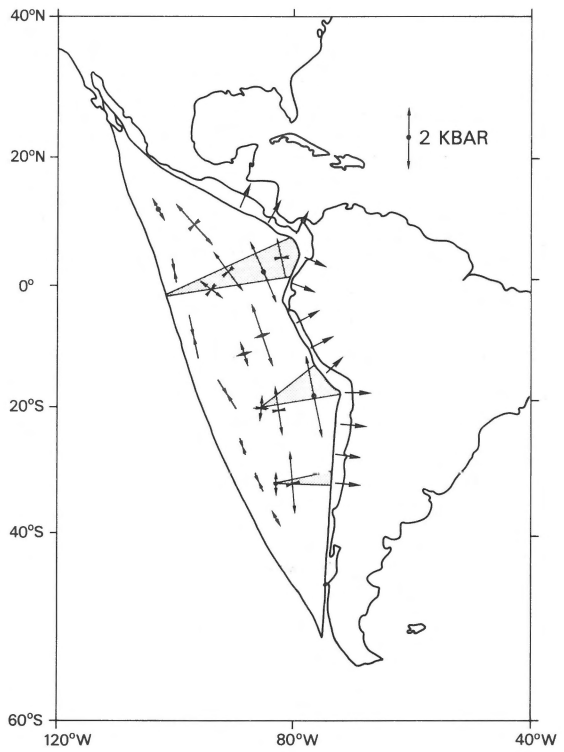

Fig. 5. The calculated stress field in the Farallon plate under the reconstructed conditions of 25–30 Ma ago, prior to the break-up into the Cocos plate and the Nacza plate. The stress values are displayed for a uniform elastic plate with a reference thickness of 100 km. Net slab forces pulling the plate towards the trench ($F_{nt}>0$) are indicated by arrows. In the trench segments without arrows resistive forces act on the Farallon plate ($F_{nt}<0$). Three zones exhibiting tensional phenomena are indicated. The northernmost one, near Panama, developed into the Cocos-Nazca spreading centre (Galapagos Rift).

Very strong support for the stress modelling procedure and our fragmentation hypothesis formulated for the Farallon plate is provided by Warsi et al. (1983). In their marine geophysical studies of the Nazca plate off Peru these authors discovered that the Mendaña Fracture zone, oriented perpen-

dicularly to the Peruvian trench (see dashed line in Fig. 6), is in an incipient stage of spreading, very much along the lines we suggested for the origin of the Cocos-Nazca spreading centre (Wortel & Cloetingh 1981, 1983).

In conclusion, lateral variations in the age of the descending lithosphere, and hence variations in F_{nt}, may be the source of significant tensional stresses in the plate to which the slab is attached. They constitute a possible cause for fragmentation of plates, in general, and of the Farallon plate, in particular.

Accretion and subduction of sediments

The process of sediment accretion at trenches has been recognized to contribute strongly to the evolution of island arcs and continents. Excellent reviews and compilations of recent work in many different regions, both offshore and onshore, are given in Leggett (1982) and Watkins & Drake (1983). A puzzling feature of observational results obtained sofar is the extremely wide variety of structures and tectonic processes encountered in the trench regions. Wortel & Cloetingh (1985) addressed this problem by considering a prominent example of a non-uniform arc or trench system, the Peru-Chile Trench. Schweller et al. (1981) have established that this trench exhibits significant lateral variations, implying *sediment accretion* in the latitude ranges 6°–19.5° S (Peru) and 27°–45° S (Central-South Chile) and *sediment subduction* in the range 19.5°–27° S (North Chile).

Schweller et al. (1981) also noted a distinct correlation between graben development on the seaward trench slope and the fate of the sediments in the trench region (see Fig. 7). This led them (following Hilde & Sharman 1978, see also Hilde 1983), to postulate the following mechanism; If the grabens are well-developed, the trench sediments can be trapped in them to then be carried down into the subduction zone along with the descending plate. If the grabens are absent (or shallow) the sediments are not (all) carried down but accrete onto the continent or island arc. Thus, the controlling factor would be the ratio of (or difference between) the transport volume of the grabens and the sediment supply, both per unit of time or rather averaged over a certain period of time.

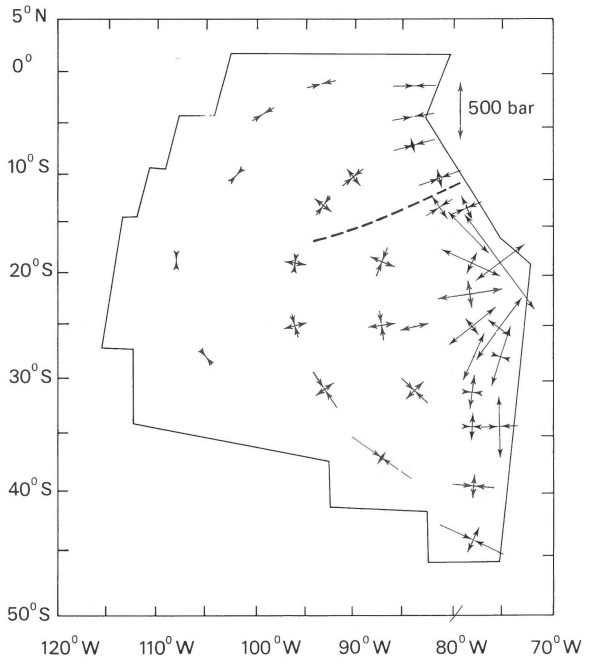

Fig. 6. Regional stress field in the Nazca plate. The solid line indicates the boundaries of the Nazca plate. The (stress) scale is indicated in the upper right-hand corner. The stress values are displayed for a uniform elastic plate with a thickness of 100 km. The dashed line indicates the position of the Mendaña Fracture Zone. After Wortel & Cloetingh (1985).

Using finite element methods Wortel & Cloetingh (1985) investigated the physical background of the graben formation, that is the stress distribution in the downbending Nazca plate. This stress distribution is dominated by the stresses associated with the bending of the plate and by the regional stress field (see Fig. 6).

To bring out the regional stress situation (Fig. 6) along the Peru-Chile Trench more clearly two stress components of the regional field are graphed in Fig. 8 for the near-trench region of the Nazca plate: $\sigma_{\perp}$ is the normal stress component in the direction normal to the trench (as a normal component it acts on a vertical plane parallel to the trench axis); $\sigma_{\parallel}$ is a normal stress component in the direction parallel to the trench axis, acting on a vertical plane perpendicular to the trench axis. The $\sigma_{\perp}$ and

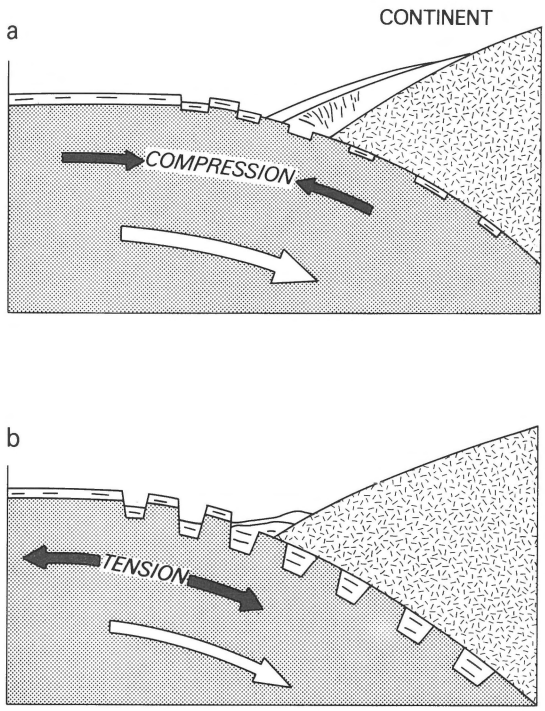

Fig. 7. Schematic cross sections of a trench region at a convergent plate boundary (after Hilde & Sharman 1978 and Schweller et al. 1981). The upper (a) and lower (b) parts of the figure illustrate the effect of regional compression and tension, respectively, on the formation of grabens on the seaward trench slope.

$\sigma_{\parallel}$-curves are shown for three models A, B and C, which differ somewhat (but all satisfy the constraint expressed in Equation 8, see Wortel & Cloetingh 1985 for details) in the distribution of the resistive forces acting on the plate. All three models exhibit the same interesting feature (for $\sigma_{\perp}$: compression normal to the trench off Peru, tension normal to the trench off North Chile and again compression along the southern part of the trench system. Such lateral changes are a direct consequence of the variations in the net subduction force F_{nt} along the trench.

The right-hand side of Fig. 8 gives the division of the Peru-Chile Trench according to Schweller et al. (1981), based on the shallow structure of the trench axis and the seaward trench slope: in provinces 1,2 and 4,5 – where grabens are absent or poorly developed – accretion occurs, whereas in province 3, with deep grabens, sediments are subducted, without any significant amount of accretion. Note that the latitude range with tension normal to the trench (positive $\sigma_{\perp}$) coincides remarkably well with the extent of province 3, where the formation of grabens is most prominent. For all stress values in Fig. 8 (as well as in Figs 5 and 6) it should be kept in mind that they are displayed for a uniform elastic plate with a reference thickness of 100 km

Along the Peru-Chile Trench neither the curvature nor the age of the (bending) Nazca plate is constant. The age variations are adequately covered by considering three cross sections with oceanic lithosphere of 15 Ma (minimum age), 40 Ma and 70 Ma old (maximum age). In Fig. 8 (and in the inset in Fig. 9) the sites where these ages are encountered are indicated. In calculating the regional stress field (Figs 6 and 8) we were essentially interested in the stress integrated over the plate's thickness. For this a uniform elastic plate model is adequate. If one is interested in the stress variation with depth, however, as in the case of bending, a depth-dependent rheology must be incorporated. Therefore, a depth- and temperature-dependent rheology (after Goetze & Evans 1979) was implemented in the models. The variations in curvature of the plate are taken from Schweller et al. (1981). Fig. 9 shows the strength distribution and the stress distribution with depth for lithosphere of the three selected ages. Two parameters of the stress distributions (see Fig. 9) are of particular interest to the formation of grabens: the depth of the neutral plane (D_{NP}, i.e. the depth at which the stress is zero; this is the maximum depth down to which the stress is tensional) and the depth down to which brittle failure takes place (D_{BF}), that is the maximum depth at which the stress equals the brittle strength in the upper part of the plate. For comparison the stress distribution in plates with the same curvature, but without regional stress field, are also graphed in Fig. 9.

As the 15 Ma cross section represents only a small part of the entire trench, the differences between the 70 Ma and the 40 Ma cross sections are most relevant. It appears that the regional stress field strongly amplifies the relatively small differences in D_{BF} due to variation in curvature and (age-dependent) thermo-mechanical structure of the

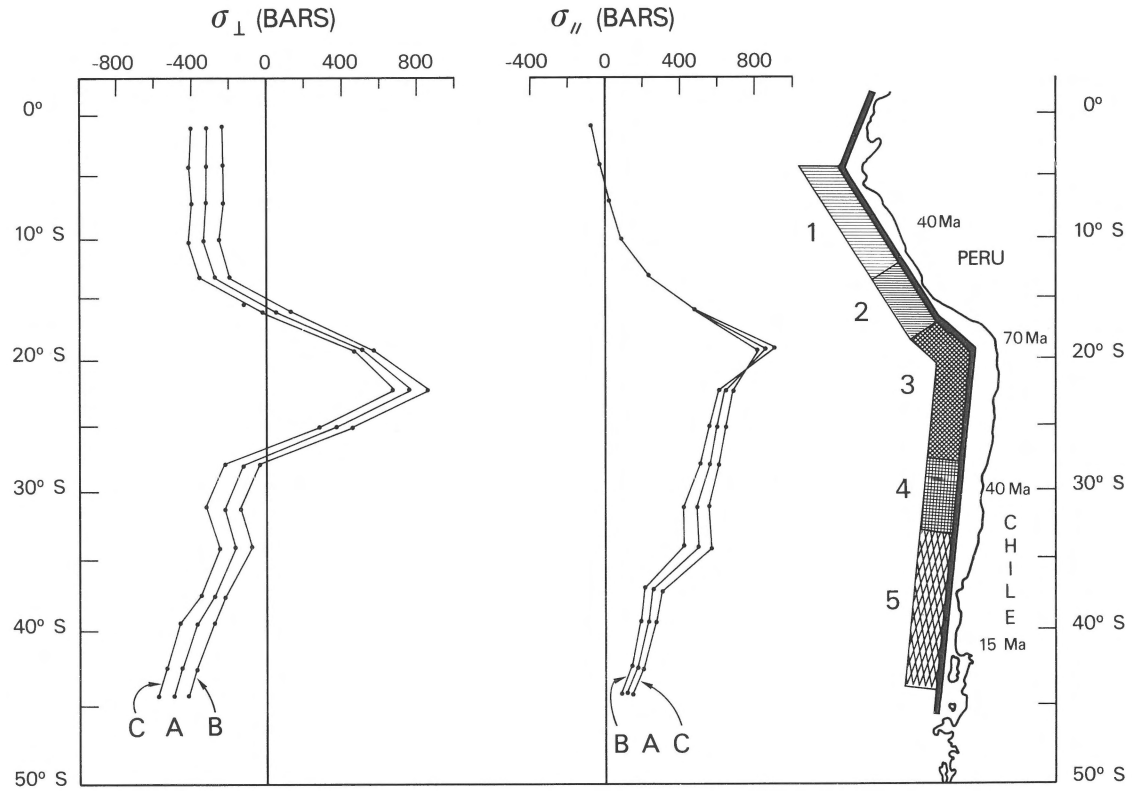

Fig. 8. $\sigma_\perp$- and $\sigma_\parallel$-values for the region near the eastern boundary of the Nazca plate along the Peru-Chile trench. Positive values indicate tension, negative values compression. $\sigma_\perp$ is the normal stress component acting in the direction perpendicular to the trench axis on a vertical plane parallel to the trench axis. $\sigma_\parallel$ is the normal stress acting in the direction parallel to the trench axis on a vertical plane perpendicular to the trench axis. Values are given for a uniform elastic plate with a reference thickness of 100 km. The curves A, B and C are labelled according to the force model used in the calculation. Model A is the preferred model. $\sigma_\parallel$ is of interest to the possible fragmentation of the Nazca plate, along fracture zones oriented roughly perpendicularly to the trench axis (see Warsi et al. 1983). The right-hand side of the figure shows the division of the Peru-Chile trench into five provinces, as made by Schweller et al. (1981). The thick black line schematically indicates the trench axis. Extensional faulting and formation of grabens (on the seaward trench slope) are most prominent in province 3. After Wortel & Cloetingh (1985).

downbending plate: D_{BF} is 20 km and 15 km for the 70 Ma and 40 Ma sections without regional stress field, respectively, and 26 km and 12 km for the same sections with regional stress field. It is of course due to the change of sign in $\sigma_\perp$ (see Fig. 8) that the role of the regional field is so pronounced. Regional tension, superimposed on the tensional bending stresses in the upper part of the plate, promotes the formation of grabens. Regional compression has the opposite effect.

A (similar) analysis of the Indonesian subduction zone, based on the regional stress field calculated by Cloetingh & Wortel (1985, 1986), is in progress. Fig. 10 (bottom part) shows the stress normal to the trench axis ($\sigma_\perp$) for segments of the Indonesian zone. The top part of the figure, after Hilde (1983), indicates that grabens are well developed in the Java part of the trench system, whereas they are 'not obvious' in the Sumatra part of the system. Again there is a close correspondence between the extent to which grabens are developed and the regional stress field, similar to the Peru-Chile Trench (see also Fig. 7).

It follows that the regional stress field plays an important role in controlling the topography of the seaward trench slope and, via the sediment trapping mechanism (Fig. 7), the process of sediment accretion onto the continental margin. Taking into

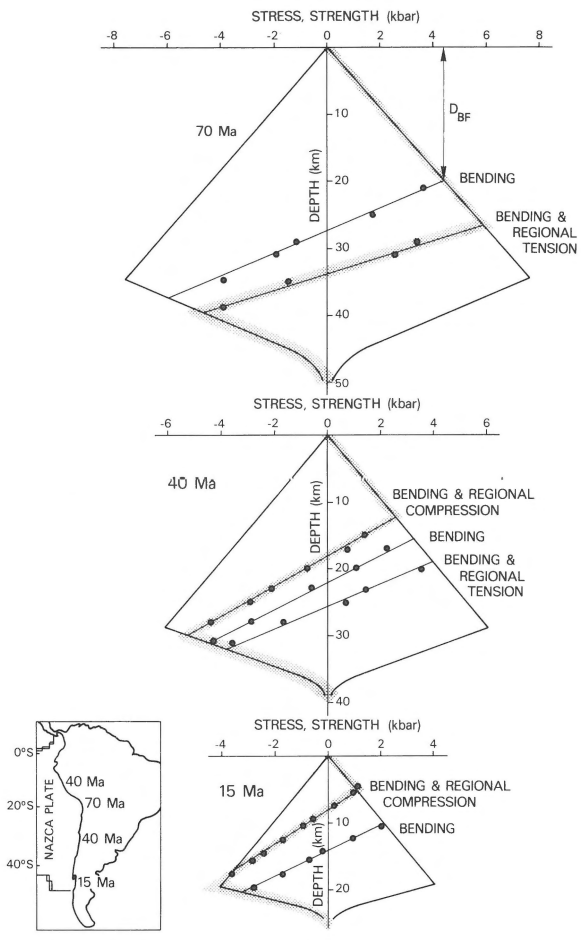

Fig. 9. Strength distributions and stress distributions in cross sections through lithosphere of 70 Ma (top), 40 Ma (middle) and 15 Ma (bottom), respectively. Sign convention: positive values indicate tension, negative values compression. Stress and also strength refer to differential stress. Solid outer lines indicate the strength envelopes. Where the stress is less than the strength the dots represent the calculated stress values. The stress distributions with shading are appropriate for the conditions along the Peru-Chile Trench. The regional stress field is taken from Fig. 8 ($\sigma_{\perp}$, model A). In addition, the stress distributions for the same sections, but without regional stress are graphed for comparison. The inset shows where lithosphere of the selected ages is encountered along the Peru-Chile Trench. D_{BF} is the maximum depth down to which brittle failure takes place. In the figure this parameter is only indicated for bending of 70 Ma old lithosphere without regional stress field.

account the role of the regional lithospheric stress field in graben formation not only explains first-order latitudinal changes in accretion and subduction of sediments in the Peru-Chile Trench, it is

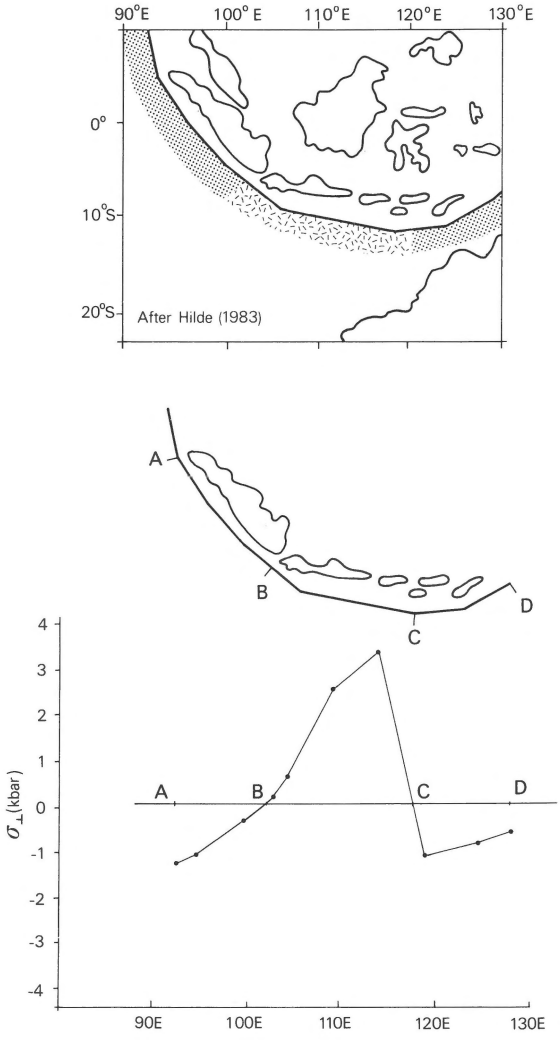

Fig. 10. Top: Lateral variations in graben development in the seaward trench slope of the Indo-Australian plate subducting in the Indonesian trench system. Symbols and denote well-developed grabens in subducting plate and areas where graben development is not obvious (after Hilde 1983). Bottom: Lateral variation of $\sigma_{\perp}$, the stress component normal to the trench axis. Sign convention: tension positive, compression negative.

also expected to contribute to understanding similar variations observed in other subduction zones.

Temporal variations in subduction dynamics with implications for vertical tectonics of active continental margins

In the two previous sections on fragmentation and

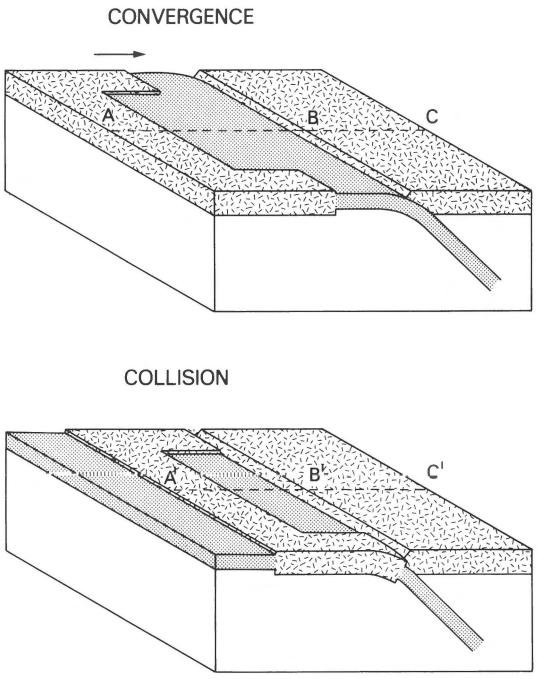

Fig. 11. Schematic diagram of two convergent plates (top), with oceanic lithosphere being consumed. Collision (bottom) gives rise to a 'land-locked' basin. No convergence takes place and the fate of the trapped oceanic lithosphere is controlled by its gravitational instability.

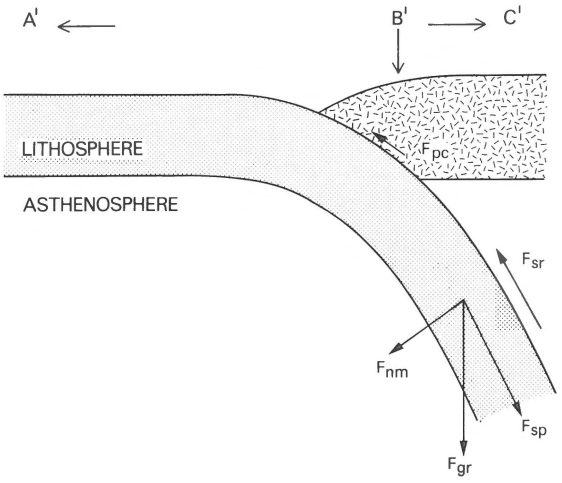

Fig. 12. Cross section along line A′B′C′ in Fig. 11. When convergence comes to an end, the velocity-dependent resistive forces F_{pc} and F_{sr} are reduced or vanish. Thus, the gravitational force on the slab effectively increases. This causes a change in shape of the bulge of the downbending lithosphere.

accretion the emphasis was on spatial variations in the subduction related forces (as in Fig. 4). Through the stress field these spatial variations induce spatial variations in tectonic processes, such as accretion. It should be noted, however, that the forces associated with subduction may not only vary spatially but also in time. Underlying causes are changes in plate geometry and changes in the age of the lithosphere at convergent plate boundaries (see Wortel & Vlaar 1978 and Wortel 1984 for such changes in the South American subduction zone). The latter changes affect the geometry of the downgoing slab (see Figs. 2 and 3) and the most important driving forces, namely the ridge push and the slab pull.

Another example of significant temporal changes in subduction dynamics is encountered at sites where plates collide (see Fig. 11). The resistive forces acting on a subducting slab mainly arise from frictional or shearing processes. They counteract the downdip component F_{sp} of the gravitational force F_{gr} acting on the slab (see Fig. 12). If the relative convergent motion of two plates comes to an end, for example in a situation depicted in Fig. 11, the resistive forces strongly decrease in magnitude or even vanish. Thus, upon cessation of plate convergence the gravitational force acting on a dipping slab effectively increases in magnitude.

In a discussion of the dynamics of 'land-locked' oceanic basins, such as shown schematically in Fig. 11, Le Pichon & Angelier (1981) and Le Pichon & Alvarez (1984) emphasized the importance of roll-back, that is the vertical motion of the subducted slab under the action of gravitational forces (component F_{nm}), leading to an oceanward migration of the trench (to the left in Fig. 12). Le Pichon and co-workers focused on the back-arc region or the overriding continental plate (between B′ and C′ in Figs 11 and 12). In this region roll-back induces extension, and hence subsidence.

Here I want to draw attention to implications of the new dynamic situations for the region near the plate contact (B′ in Figs 11 and 12) and the area seaward of the trench (A′-B′ in Figs 11 and 12). Of interest here is that the flexure of the oceanic lithosphere not only migrates away from the former overriding plate but, in addition, changes in shape. The effective increase in gravitational force

acting on the slab induces an increase in curvature of the plate, thereby producing a higher 'bulge', seaward of the trench. Numerical calculations (Wortel & Cloetingh, in prep.) show that, depending on the age of the trapped oceanic lithosphere, vertical movements may be induced over distances of 100–200 km from the trench (between A′ and B′, Figs 11 and 12). Near the plate contact this may have serious tectonic effects (vertical motion, tilting), whereas farther away from the plate contact the magnitude may still be relevant in the context of sea level fluctuations (see also Cloetingh 1986).

Of special interest in this specific situation are the timescales involved. The vertical motion induced upon collision is controlled by the timescale of the collision process. The decay of the induced motion, however, is determined by the processes which govern the evolution of the subducted slab after termination of subduction. Primarily these processes are of thermal origin, which implies a timescale in the order of 10 Ma or several tens of million years. This is likely to be longer (but not necessarily so) than the timescale of the process which caused the cessation of subduction.

Conclusions

A local balance between slab pull force and resistive forces acting on a subducted slab is not a standard feature of the dynamics of the lithosphere. Generally, the slab pull force is either partially compensated or over-compensated. Partial or over-compensation of the slab pull force implies a net force transmitted from the subducted slab to the lithospheric plate to which the slab is attached. This net force, and in particular the way it varies along the convergent plate boundary, strongly affects the regional stress field in the lithosphere. This spatially varying stress field is subject to temporal variations, through the dependence of the main plate tectonic (driving) forces on the age of the lithosphere near the trench. Taking account of the slab pull being compensated and of the effect of this on the lithospheric stress field sheds light on several, hitherto unexplained spatial and temporal variations in tectonic processes (plate fragmentation, accretion and subduction of sediments, vertical tectonics of active continental margins).

Acknowledgment

I thank Prof. Dr. N. J. Vlaar and Dr. Sierd Cloetingh for stimulating cooperation and for their important contributions to the research described in this paper.

References

Backus, G., J. Park & D. Garbasz 1981 On the relative importance of the driving forces of plate motion – Geophys. J.R. Astron. Soc. 67: 415–435

Chapple, W.M. & T.E. Tullis 1977 Evaluation of the forces that drive the plates – J. Geophys. Res. 82: 1967–1984

Cloetingh, S.A.P.L. 1982 Evolution of passive continental margins and initiation of subduction zones – PhD–Thesis, University of Utrecht, 111 pp

Cloetingh, S. 1986 Tectonics of passive margins: implications for the stratigraphic record – Geol. Mijnbouw 65: xxx–xxx (this issue)

Cloetingh, S. & R. Wortel 1985 Regional stress field of the Indian plate – Geophys. Res. Lett. 12: 77–80

Cloetingh, S. & R. Wortel in press Stress in the Indo-Australian plate – Tectonophysics

Elsasser, W.M. 1967 Convection and stress propagation in the upper mantle – Princeton Univ. Tech. Rep. 5, 65 pp

England, P. & R. Wortel 1980 Some consequences of the subduction of young lithosphere – Earth Planet. Sci. Lett. 47: 403–415

Forsyth, D. & S. Uyeda 1975 On the relative importance of the driving forces of plate motion – Geophys. J.R. Astron. Soc. 43: 163–200

Goetze, C. & B. Evans 1979 Stress and temperature in the bending lithosphere as constrained by experimental rock mechanics – Geophys. J.R. Astron. Soc. 59: 463–478

Hey, R. 1977 Tectonic evolution of the Cocos-Nazca preading center – Geol. Soc. Am. Bull. 88: 1404–1420

Hilde, T.W.C. 1983 Sediment subduction versus accretion around the Pacific – Tectonophysics 99: 381–397

Hilde, T.W.C. & G.F. Sharman 1978 Fault structure of the descending plate and its influence on the subduction process – EOS, Trans. Am. Geophys. Union 59: 1182

Leggett, J.K. (Editor) 1982 Trench-forearc geology: Sedimentation and tectonics on modern and ancient active plate margins – Geol. Soc. London Spec. Publ. No. 10, Blackwell, Oxford: 576 pp

Le Pichon, X. & J. Angelier 1981 The Aegean Sea – Phil. Trans. R. Soc. London A300: 357–372

Le Pichon, X. & F. Alvarez 1984 From stretching to subduction in back-arc regions: dynamic considerations – Tectonophysics 102: 343–357

Lister, C.R.B. 1975 Gravitational drive on oceanic plates caused by thermal contraction – Nature 257: 663–665

McKenzie, D.P. 1969 Speculations on the consequences and causes of plate motion – Geophys. J.R. Astron. Soc. 18: 1–32

McKenzie, D.P. 1970 Temperature and potential temperature beneath island arcs – Tectonophysics 10: 357–366

Oxburgh, R. & E.M. Parmentier 1977 Compositional and density stratification in oceanic lithosphere – J. Geol. Soc. London 133: 343–355

Ruff, L. & H. Kanamori 1980 Seismicity and the subduction process – Phys. Earth. Planet. Inter. 23: 240–252

Schweller, W.J., L.D. Kulm & R.A. Prince 1981 Tectonics, structure and sedimentary framework of the Peru–Chile Trench – Geol. Soc. Am. Memoir 154: 323–349

Vlaar, N.J. 1975 The driving mechanism of plate tectonics. In: Borradaile, G.J. et al. (Eds.): Progress in Geodynamics, North-Holland, Amsterdam: 234–245

Vlaar, N.J. & M.J.R. Wortel 1976 Lithospheric aging, instability and subduction – Tectonophysics 32: 331–351

Warsi, W.E.K., T.W.C. Hilde & R.C. Searle 1983 Convergence structures of the Peru Trench between 10° S and 14° S – Tectonophysics 99: 313–329

Watkins, J.S. & C.L. Drake (Editors) 1983 Studies in continental margin geology – AAPG Memoir No. 34, Am. Assoc. Petrol. Geol., Tulsa (Okla.): 801 pp

Wortel, M.J.R. 1980 Age-dependent subduction of oceanic lithosphere – PhD-Thesis, University of Utrecht, 147 pp

Wortel, R. 1982 Seismicity and the rheology of subducted slabs – Nature 296: 553–556

Wortel, M.J.R. 1984 Spatial and temporal variations in the Andean subduction zone – J. Geol. Soc. London 141: 783–791

Wortel, R. 1986 Deep earthquakes and the thermal assimilation of subducting lithosphere – Geophys. Res. Lett. 13: 34–37

Wortel, R. & S. Cloetingh 1981 On the origin of the Cocos–Nazca spreading center – Geology 9: 425–430

Wortel, R. & S. Cloetingh 1983 A mechanism for the fragmentation of oceanic plates AAPG Memoir 34: 793 801

Wortel, M.J.R. & S.A.P.L. Cloetingh 1985 Accretion and lateral variations in tectonic structure along the Peru-Chile Trench – Tectonophysics 112: 443–462

Wortel, M.J.R. & N.J. Vlaar 1978 Age-dependent subduction of oceanic lithosphere beneath western South America – Phys. Earth Planet. Inter. 17: 201–208